PHYSICAL REVIEW D **94,** 053008 (2016)

Implications of lepton flavor violation on long baseline neutrino oscillation experiments

Soumya C. and R. Mohanta

School of Physics, University of Hyderabad, Hyderabad 500 046, India

(Received 5 May 2016; published 19 September 2016)

Nonstandard neutrino interactions (NSIs), the subleading effects in the flavor transitions of neutrinos, play a crucial role in the determination of the various unknowns in neutrino oscillations, such as neutrino mass hierarchy, the Dirac CP violating phase, and the octant of the atmospheric mixing angle. In this work, we focus on the possible implications of lepton flavor violating (LFV) NSIs, which generally affect the neutrino propagation, on the determination of these unknown oscillation parameters. We study the effect of these NSIs on the physics potential of the currently running and upcoming long-baseline experiments, i.e., T2K, NOνA, and DUNE. We also check the allowed oscillation parameter space in the presence of LFV NSIs.

DOI: 10.1103/PhysRevD.94.053008

I. INTRODUCTION

Neutrino oscillation [1–7], the phenomenon of the flavor transition of neutrinos, provides strong evidence for neutrino mass and mixing. Further, the three-flavor neutrino oscillation model has become a very successful theoretical framework, which could accommodate almost all neutrino oscillation experimental data except for some results in very short baseline experiments. However, some of the oscillation parameters [8,9] (Dirac CP violating phase, neutrino mass hierarchy, and the octant of the atmospheric mixing angle) in the standard paradigm are still not known. Recently, the Daya Bay [10,11], RENO [12], and Double CHOOZ [13] experiments have observed that the value of the reactor mixing angle is significantly large (close to its upper bound), which improves the sensitivities to determine these unknowns by enhancing the matter effect. Therefore, a good understanding of subleading contributions to neutrino oscillation, coming from various new physics scenarios, may lead to the enhancement of the physics potential of long-baseline neutrino oscillation experiments.

Nonstandard neutrino interactions (NSIs) [14,15] can be considered as subleading effects in the neutrino oscillations, which arise from various new physics scenarios beyond the standard model. The NSIs, which come from neutral current (NC) interactions, can affect the propagation of neutrino, whereas NSIs coming from the charged current (CC) interactions of neutrinos with quarks and leptons can affect the production and detection processes of neutrinos. However, in this work, we consider only the NSIs which affect the propagation of neutrinos. The Lagrangian that corresponds to NSIs during the propagation is given by [16]

$$\mathcal{L}_{\rm NSI} = -2\sqrt{2}G_F\varepsilon^{fC}_{\alpha\beta}(\bar{\nu}_\alpha\gamma^\mu P_L\nu_\beta)(\bar{f}\gamma_\mu P_C f), \qquad (1)$$

where G_F is the Fermi coupling constant, $\varepsilon^{fC}_{\alpha\beta}$ are the new coupling constants, the so-called NSI parameters, f is the fermion, and $P_C = (1 \pm \gamma_5)/2$ are the right ($C = R$) and left ($C = L$) chiral projection operators. The NSI contributions which are relevant as neutrinos propagate through the earth are those coming from the interaction of the neutrino with e, u, and d because the earth matter is made up of these fermions only. Therefore, the effective NSI parameter is given by

$$\varepsilon_{\alpha\beta} = \sum_{f=e,u,d}\frac{n_f}{n_e}\varepsilon^f_{\alpha\beta}, \qquad (2)$$

where $\varepsilon^f_{\alpha\beta} = \varepsilon^{fL}_{\alpha\beta} + \varepsilon^{fR}_{\alpha\beta}$, n_f is the number density of the fermion f and n_e is the number density of the electrons in earth. For earth matter, we can assume that the number densities of electrons, protons, and neutrons are equal, i.e., $n_n \approx n_p = n_e$, which implies that $n_u \approx n_d = 3n_e$.

NSIs and their consequences have been studied quite extensively in the literature both in model-dependent (mass models) and -independent ways. Furthermore, there are studies which have been done to investigate the effect of NSIs on atmospheric neutrinos [17–19], solar neutrinos [20–24], accelerator neutrinos [25–35], and supernova neutrinos [36–38]. However, it is very crucial to understand the implications of new physics effects at the long-baseline experiments like T2K, NOνA, and DUNE. In this regard, there are many recent works which have discussed the various aspects of NSIs at long-baseline experiments [39–41]; for instance, in [42], the authors have obtained the constraints on NSI parameters using long-baseline experiments and, in [43], the authors have discussed the degeneracies among the oscillation parameters in the presence of NSIs. However, in this paper, we focus on the effect of the lepton flavor violating NSIs on the

determination of various unknowns at long-baseline experiments.

We have discussed the physics potential of long-baseline experiments in our previous papers [44,45]. Since neutrino oscillation physics has already entered its precision era, one should take care of various subleading effects such as NSIs in the oscillation physics. In this regard, we would like to study the effect of the lepton flavor violating NSIs on the determination of oscillation parameters. This paper is organized as follows. In Sec. II, we discuss the basic formalism of neutrino oscillation including NSI effects. In Sec. III, we study the effect of NSI parameters on ν_e appearance oscillation probability. The effect of LFV NSI on the physics potential of long-baseline experiments is discussed in Sec. IV. In Sec. V, we discuss the parameter degeneracies among the oscillation parameters in the presence of NSIs. Section VI contains the summary and conclusions.

II. NEUTRINO OSCILLATION WITH NSIS

In the standard oscillation (SO) paradigm, the propagation of neutrinos through matter is described by the Hamiltonian,

$$H_{\rm SO} = H_0 + H_{\rm matter} = \frac{1}{2E} U \cdot \mathrm{diag}(0, \Delta m^2_{21}, \Delta m^2_{31}) \cdot U^\dagger + \mathrm{diag}(V_{CC}, 0, 0), \tag{3}$$

where the H_0 is the Hamiltonian in vacuum, $\Delta m^2_{ji} = m^2_j - m^2_i$ is the neutrino mass squared difference, $H_{\rm matter}$ is the Hamiltonian responsible for the matter effect, $V_{CC} = \sqrt{2} G_F n_e$ is the matter potential, and U is the Pontecorvo-Maki-Nakagawa-Sakata mixing matrix which is described by three mixing angles (θ_{12}, θ_{13}, θ_{23}) and one phase (δ_{CP}) and is given by

$$U_{PMNS} = \begin{pmatrix} c_{12}c_{13} & s_{12}c_{13} & s_{13}e^{-i\delta} \\ -s_{12}c_{23} - c_{12}s_{13}s_{23}e^{i\delta} & c_{12}c_{23} - s_{12}s_{13}s_{23}e^{i\delta} & c_{13}s_{23} \\ s_{12}s_{23} - c_{12}s_{13}c_{23}e^{i\delta} & -c_{12}s_{23} - s_{12}s_{13}c_{23}e^{i\delta} & c_{13}c_{23} \end{pmatrix}, \tag{4}$$

with $c_{ij} = \cos\theta_{ij}$ and $s_{ij} = \sin\theta_{ij}$. The NSI Hamiltonian, which is coming from the interactions of neutrinos as they propagate through matter, is given by

$$H_{NSI} = V_{CC} \begin{pmatrix} \varepsilon_{ee} & \varepsilon_{e\mu} & \varepsilon_{e\tau} \\ \varepsilon^*_{e\mu} & \varepsilon_{\mu\mu} & \varepsilon_{\mu\tau} \\ \varepsilon^*_{e\tau} & \varepsilon^*_{\mu\tau} & \varepsilon_{\tau\tau} \end{pmatrix}, \tag{5}$$

where $\varepsilon_{\alpha\beta} = |\varepsilon_{\alpha\beta}| e^{i\delta_{\alpha\beta}}$ are the complex NSI parameters, which give the coupling strength of nonstandard interactions. The off-diagonal elements of the NSI Hamiltonian ($\varepsilon_{e\mu}$, $\varepsilon_{e\tau}$ and $\varepsilon_{\mu\tau}$) are the lepton flavor violating NSI parameters, which are our subject of interest.

Almost all current neutrino oscillation data are consistent with the standard oscillation paradigm. Therefore, the effect of NSI on the oscillation phenomena is expected to be very small. Moreover, some neutrino mass models—for instance, the triplet seesaw model [46] and Zee Babu model [47]—predict the value of NSI parameters of the order of 10^{-4}–10^{-3}, which depends on the scale of new physics and the neutrino mass ordering. The strong constraints on NSI parameters make them very difficult to be observed in the long-baseline experiments. Therefore, we use a phenomenological approach to study the effect of NSIs on the physics potential of such experiments. The model-independent current upper bounds of NSI parameters at 90% C.L. are given as [48,49]

$$|\varepsilon_{\alpha\beta}| < \begin{pmatrix} 4.2 & 0.3 & 0.5 \\ 0.3 & 0.068 & 0.04 \\ 0.5 & 0.04 & 0.15 \end{pmatrix}. \tag{6}$$

From the above equation, it should be noted that the bound on LFV-NSI parameters is $|\varepsilon_{e\mu}| < 0.3$, $|\varepsilon_{\mu\tau}| < 0.04$, and $|\varepsilon_{e\tau}| < 0.5$; therefore, in our analysis, we use the representative values for $\varepsilon_{e\mu}$, $\varepsilon_{\mu\tau}$, and $\varepsilon_{e\tau}$ close to their upper bounds, i.e., as 0.2, 0.03, and 0.3, respectively. It should also be noted that each NSI parameter $\varepsilon_{\alpha\beta}$ has a CP phase $\delta_{\alpha\beta}$, which can vary between $-\pi$ and π.

III. LFV-NSI EFFECT ON ν_e APPEARANCE PROBABILITY

In general, the measurement of branching ratios (BRs) and the CP violation parameters can be used to probe the new physics effects or nonstandard interactions in the flavor sector. If any inconsistency were found between the experimental observed values and the corresponding SM predictions in these observables, it would imply the presence of new physics. However, in the case of neutrinos, one cannot use branching ratio measurements to study the new physics effects, since the mass difference between neutrinos is really small and also experiments detect neutrinos as flavor states (mixed state of mass eigenstates). The various issues regarding the BR measurement of neutrinos are discussed in [50]. Therefore, in the case of

TABLE I. The experimental specifications.

Exp. setup	T2K [56–58]	NOνA [59–61]	DUNE [62,63]
Detector	Water Cherenkov	Scintillator	Liquid argon
Beam power (MW)	0.75	0.77	0.7
Fiducial mass (kt)	22.5	14	35
Baseline length (km)	295	810	1300
Running time (yrs)	5 $(3\nu + 2\bar{\nu})$	6 $(3\nu + 3\bar{\nu})$	10 $(5\nu + 5\bar{\nu})$

neutrinos, the new physics effect can be studied by using the oscillation probabilities. The super-beam experiments like T2K, NOνA, and DUNE use muon neutrino beams as the neutrino source. Therefore, in this section, we discuss the consequences of LFV-NSI parameters on neutrino appearance ($\nu_\mu \to \nu_e$) probability.

We use the GLoBES package [51,52] along with the Snu plugin [53,54] for our analysis to study the implications of LFV-NSI on the propagation of neutrinos. The experimental details of T2K, NOνA, and DUNE that we consider in this analysis are given in Table I. The values of standard oscillation parameters that we use in the analysis are given in Table II.

For an illustration, we show the calculated transition probability with and without NSI for T2K (top panel), NOνA (middle panel), and DUNE (bottom panel) by assuming hierarchy as NH in Fig. 1 for neutrinos. In the figure, the light shaded regions correspond to probability in the standard oscillation (SO) paradigm, whereas the dark shaded green, red, and blue regions represent the additional contribution to the oscillation probability, which are coming from NSI parameters $\varepsilon_{e\mu}$, $\varepsilon_{\mu\tau}$, and $\varepsilon_{e\tau}$, respectively. From the figure, we can see that the NSI contribution to oscillation probability is noteworthy in the presence of $\varepsilon_{e\tau}$ and $\varepsilon_{e\mu}$ parameters, whereas the contribution from $\varepsilon_{\mu\tau}$ is negligible. It can also be seen from the figure that there is significant change in the oscillation probability in the presence of NSIs for both NOνA and DUNE, whereas for T2K, the effect is found to be rather small; i.e., NOνA and DUNE are more sensitive to NSI effects. We can also see that there is a substantial change in the oscillation probability of the DUNE experiment in the presence of NSI. Therefore, the DUNE experiment can be used to investigate various effect of NSI, which are expected to be observed in the long-baseline experiment. Moreover, NSI can even affect the results, which require much precision on their measurements for the determination of the unknowns in the neutrino sector of the currently running experiments like T2K and NOνA.

TABLE II. The true values of oscillation parameters considered in the simulations are taken from [64].

Oscillation parameter	True value
$\sin^2\theta_{12}$	0.32
$\sin^2 2\theta_{13}$	0.1
$\sin^2\theta_{23}$	0.5, 0.41 (LO), 0.59 (HO)
$\Delta m^2_{\rm atm}$	2.4×10^{-3} eV^2 for NH
	-2.4×10^{-3} eV^2 for IH
Δm^2_{21}	7.6×10^{-5} eV^2
δ_{CP}	0°

IV. NSI EFFECT ON THE PHYSICS POTENTIAL OF LONG-BASELINE EXPERIMENTS

The primary objective of long-baseline experiments is the determination of the various unknowns (neutrino mass ordering, *CP* violating phase, and octant of the atmospheric mixing angle) in the phenomenon of neutrino oscillation. In this section, we discuss the effect of LFV-NSI on the determination of these unknowns. From the previous section, we found that the NSI parameter $\varepsilon_{e\tau}$ can significantly change the oscillation probability. Therefore, for simplicity, we focus on the effect of $\varepsilon_{e\tau}$ on the determination of other unknowns in neutrino oscillation sector. We also compare the effect of NSIs on the physics potential of different experiments that have been considered in this paper. All the sensitivities are computed by using GLoBES.

A. Effect on the determination of neutrino mass ordering

So far, we do not know whether the hierarchy of the neutrino mass is normal ($m_1 < m_2 \ll m_3$) or inverted ($m_3 \ll m_1 < m_2$). The MSW effect, the so-called matter effect, plays a crucial role in the determination of neutrino mass hierarchy because, unlike vacuum oscillation, it gives different contributions to the oscillation probability for NH and IH as one can see from the top panel of Fig. 2. Therefore, a thorough study of the effect of NSIs on the determination of MH is of great importance in oscillation physics.

However, if we compare the top and bottom panels of Fig. 2, we can see that there is considerable overlap between the hierarchies in the presence of NSIs, and this overlap will worsen the hierarchy determination capability of long-baseline experiments. Further, the MH sensitivity as a function of true values of Dirac *CP* phase δ_{CP} is shown in Fig. 3. In the figure, the solid blue line corresponds to the MH sensitivity in SO, which is obtained by comparing true event spectrum as NH and test event spectrum as IH. The blue band in the figure shows the variation in MH sensitivity for different values of $\delta_{e\tau}$ with $\varepsilon_{e\tau} = 0.3$. In all cases, we do marginalization over SO parameters in their allowed parameter space and add a prior on $\sin^2 2\theta_{13}$. From the figure, it is clear that though the presence of NSI worsens MH sensitivity, there is a possibility to determine mass hierarchy for T2K (NOνA) above 2σ (3σ) for 30% (75%) of parameter space of δ_{CP}.

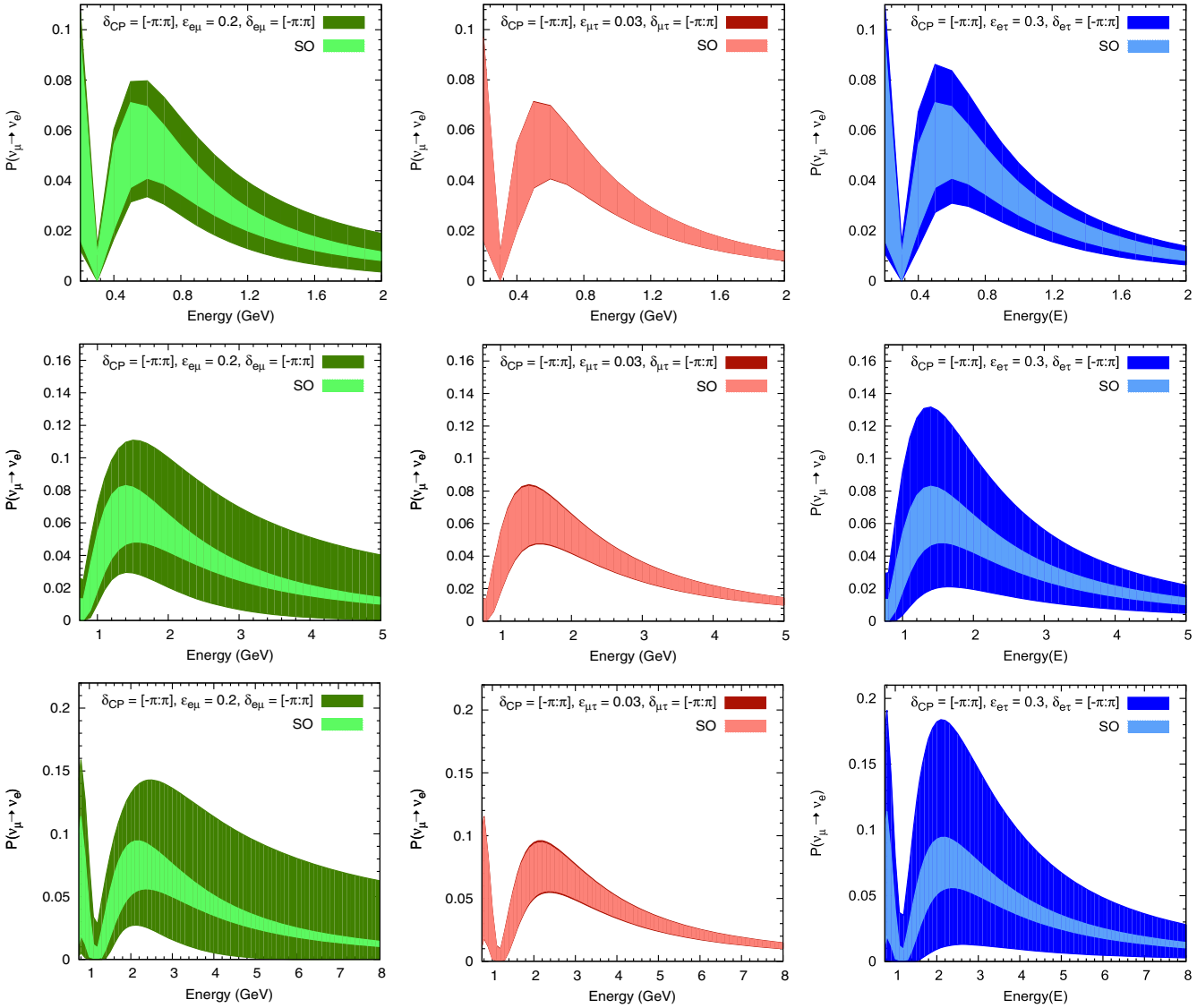

FIG. 1. Neutrino appearance probability for the $\nu_\mu \to \nu_e$ without NSI (light shaded region) and with NSI (dark shaded green, red, and blue regions correspond to $\varepsilon_{e\mu}$, $\varepsilon_{\mu\tau}$, and $\varepsilon_{e\tau}$ parameter contributions, respectively) for T2K (top panel), NOνA (middle panel), and DUNE (bottom panel). The hierarchy is assumed to be NH.

B. Effect on the determination of octant of θ_{23}

The precision measurements of atmospheric neutrino oscillation data by the Super-Kamiokande experiment prefer a maximal mixing of θ_{23}, i.e., $\theta_{23} = \pi/4$. However, disappearance measurements of MINOS [55] point towards nonmaximal mixing, which contradicts the measurements of Super-Kamiokande. Therefore, there are two possibilities—either $\theta_{23} < \pi/4$, the so-called lower octant (LO), or $\theta_{23} > \pi/4$, the so-called higher octant (HO). The T2K disappearance measurement, which provides the most precise value of θ_{23}, indicates that θ_{23} is near to maximal. However, T2K data along with reactor data show that θ_{23} is in a higher octant. The resolution of such tension between LO and HO of the atmospheric mixing angle is one of the challenging goals of long-baseline neutrino oscillation experiments. In this section, we discuss the effect of LFV-NSI on the resolution of the octant of the atmospheric mixing angle.

The octant degeneracy is merely a consequence of the inherent structure of three-flavor neutrino oscillation probability, where a set of oscillation parameters gives disconnected regions in neutrino oscillation parameter space and this makes it too difficult to find the true solution. However, the matter effect in long-baseline experiments can help to resolve the octant of θ_{23} [65] since the oscillation probability gives different contributions to HO and LO as one can see from the upper panels of Fig. 4. From the lower panels of the figure, it can be seen that there is considerable overlap between the lower and higher octants in the presence of LFV-NSI, which will

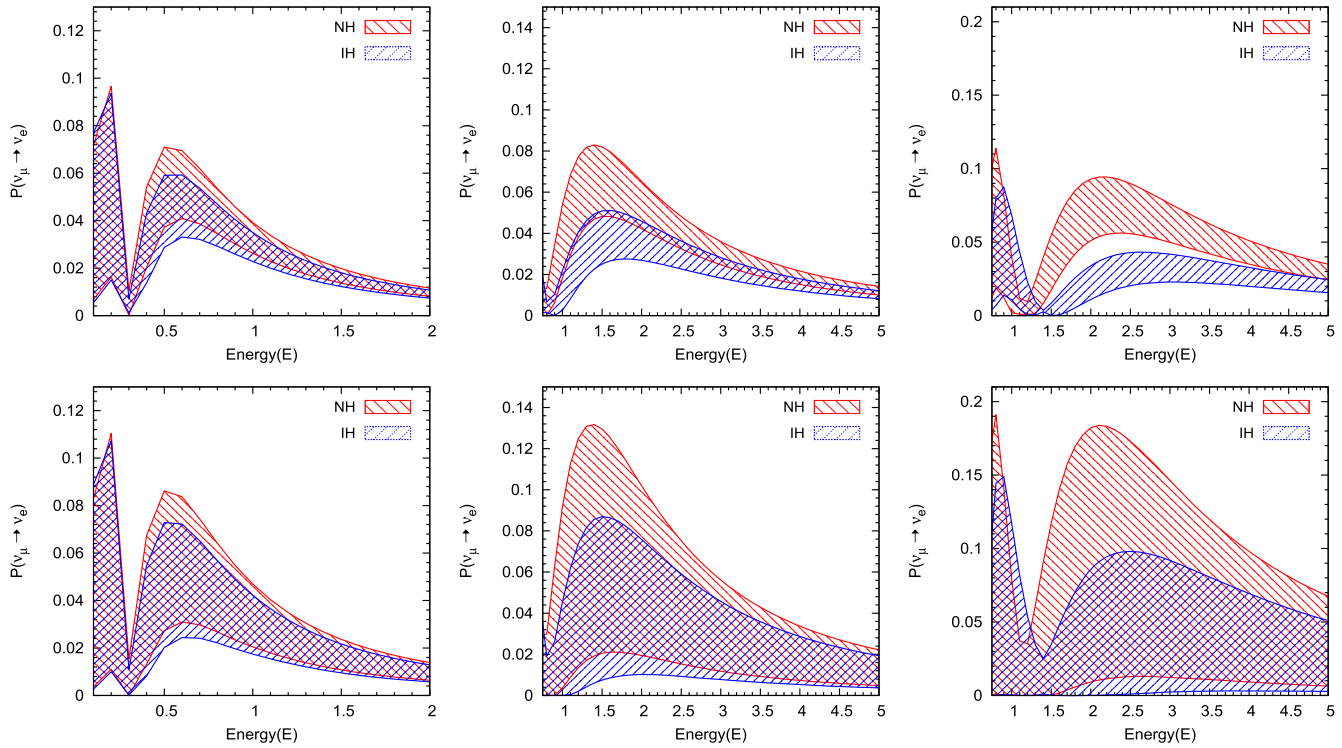

FIG. 2. Neutrino appearance probability for the $\nu_\mu \to \nu_e$ without NSI (top panel) and with NSI (bottom panel) by assuming both NH (red) and IH (blue) for T2K (left panel), NOνA (middle panel), and DUNE (right panel).

worsen the sensitivity of long-baseline experiments in the determination of octant of θ_{23}. Moreover, the octant sensitivity as a function of the true value of $\sin^2\theta_{23}$ is given in Fig. 5. The octant sensitivity is obtained by comparing the true event spectrum (HO/LO) with the test event spectrum (LO/HO). While calculating the χ^2, we do a marginalization over SO parameter space in their allowed values and add a prior on $\sin^2 2\theta_{13}$. From the figure, we can see that there is a possibility of enhancement in the sensitivity of the octant of the atmospheric mixing angle in the presence of LFV-NSIs, though LFV-NSIs worsen the sensitivity.

C. Effect on the determination of *CP* violating phase δ_{CP}

One of the main objectives of long-baseline neutrino oscillation experiments is the determination of the *CP* violation (CPV) in the leptonic sector. Therefore, it is crucial to study the effect of NSI on the determination of CPV at T2K, NOνA, and DUNE experiments. The direct measurement of *CP* violation can be obtained by looking at the difference in the transition probability of *CP* conjugate channels, i.e., by analyzing the ν_e appearance and $\bar{\nu}_e$ appearance probabilities.

We use the observable so-called *CP* asymmetry (A_{CP}) to quantify the effects due to *CP* violation, and it is defined as

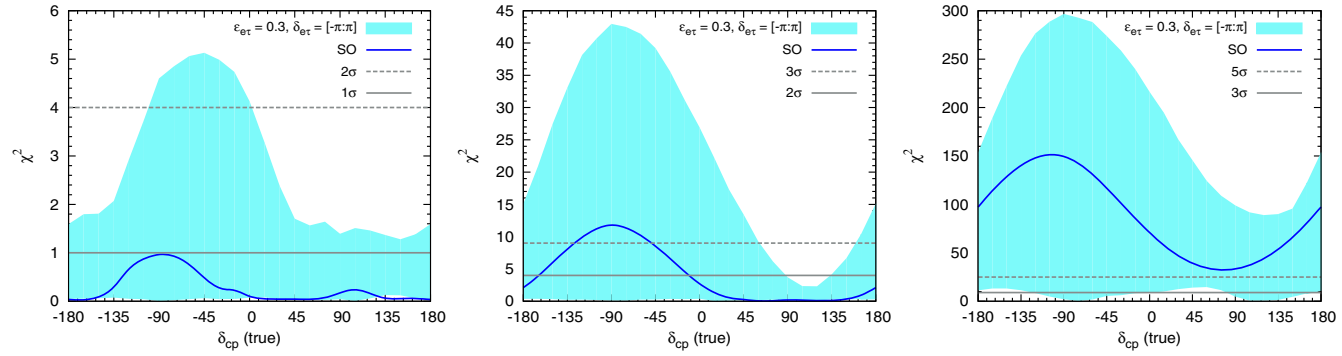

FIG. 3. Mass hierarchy sensitivity as a function of true values of δ_{CP}. The blue solid line in the figure corresponds to MH sensitivity without NSI, whereas the blue band in the figure shows the MH sensitivity in the presence of NSI ($\varepsilon_{e\tau} = 0.3$) in the allowed range of $\delta_{e\tau}$ for T2K (left panel), NOνA (middle panel), and DUNE (right panel).

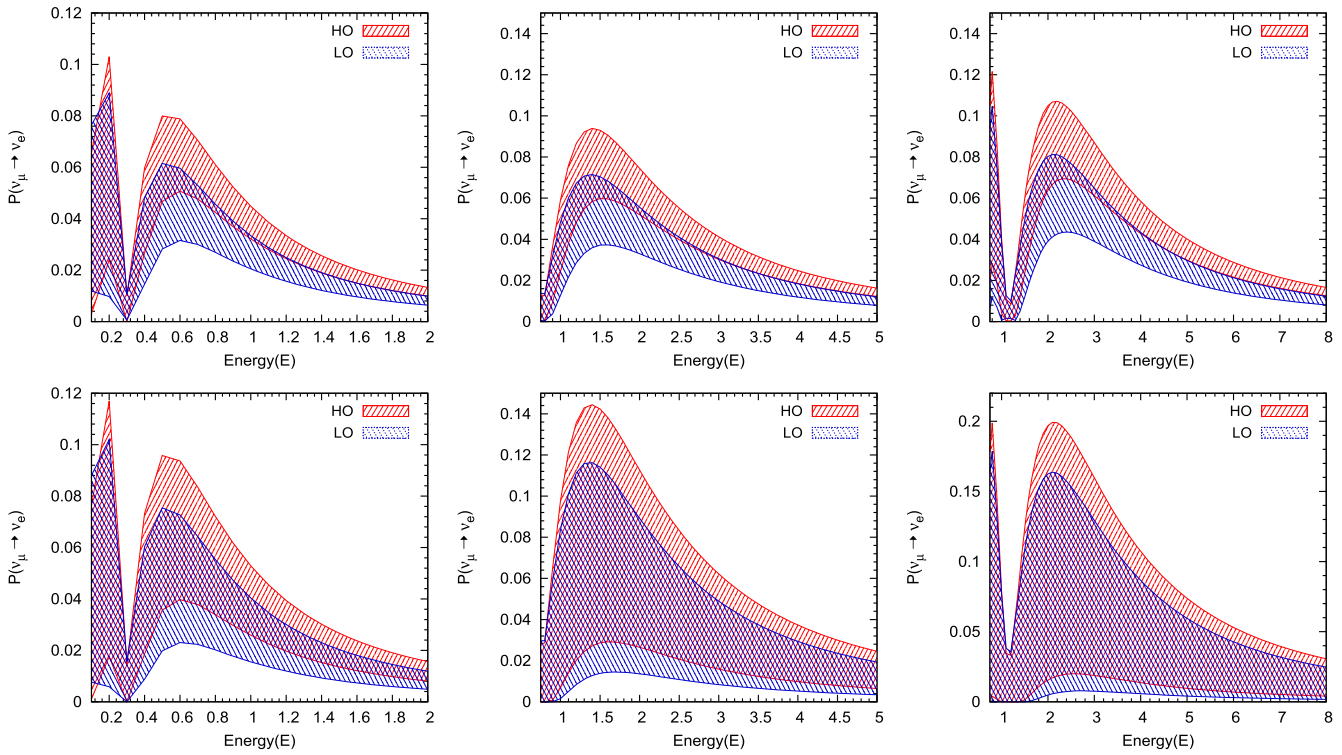

FIG. 4. Neutrino appearance probability for the $\nu_\mu \to \nu_e$ without NSI (top panel) and with NSI (bottom panel) by assuming both HO (red) and LO (blue) for T2K (left panel), NOνA (middle panel), and DUNE (right panel).

$$A_{CP} = \frac{P_{\mu e} - \bar{P}_{\mu e}}{P_{\mu e} + \bar{P}_{\mu e}}, \tag{7}$$

where $P_{\mu e}$ is the ν_e appearance probability and $\bar{P}_{\mu e}$ is the $\bar{\nu}_e$ appearance probability. Figure 6 shows the CP asymmetry bands for T2K (left panel), NOνA (middle panel), and DUNE (right panel) without NSI (light colored band) and with NSI (dark colored band) by assuming both normal (top panel) and inverted (bottom panel) hierarchies. The solid black line corresponds to CP asymmetry for $\delta_{CP} = 0$ without NSI, whereas the dashed white line corresponds to CP asymmetry for $\delta_{CP} = 0$ with NSI ($\varepsilon_{e\tau} = 0.3$). The dark bands in the figure show the impact of the phase of LFV-NSI parameter on A_{CP}. Therefore, the dark bands correspond to the fake CP signals which are coming from NSI. From the figures, we can see that there is not much change in the asymmetry with NSI and without NSI in the case of T2K, whereas in the case of NOνA, the bands show that there is significant change in the asymmetry with NSI and without NSI. Moreover, the change in the asymmetry is quite large in the case of DUNE. From the figure, it is clear that NSI can give fake CP signals even without considering contributions from the intrinsic phase ($\delta_{e\tau}$) of the NSI

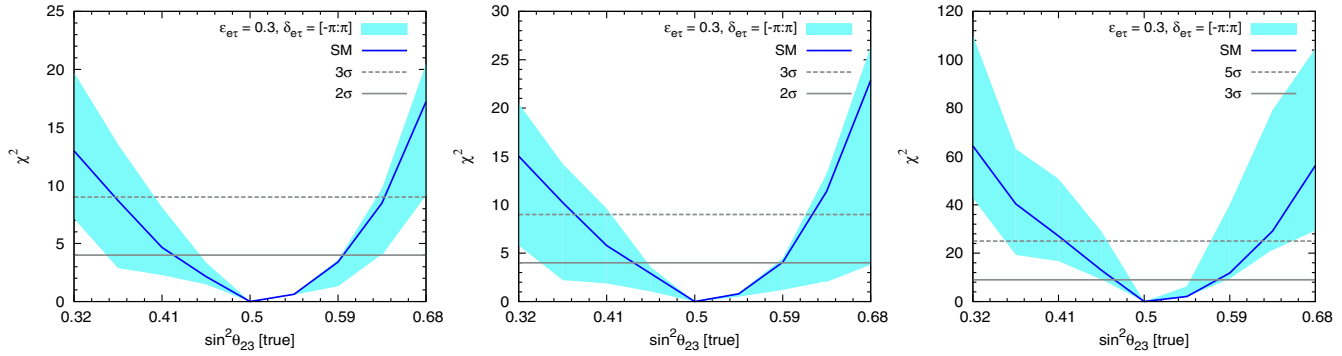

FIG. 5. Octant sensitivity as a function of true values of $\sin^2\theta_{23}$. The blue line in the figure corresponds to the octant without NSI, whereas the light blue band in the figure shows the octant sensitivity in the presence of NSI ($\varepsilon_{e\tau} = 0.3$) in the allowed range of $\delta_{e\tau}$ for T2K (left panel), NOνA (middle panel), and DUNE (right panel). Neutrino MH is assumed to be normal hierarchy.

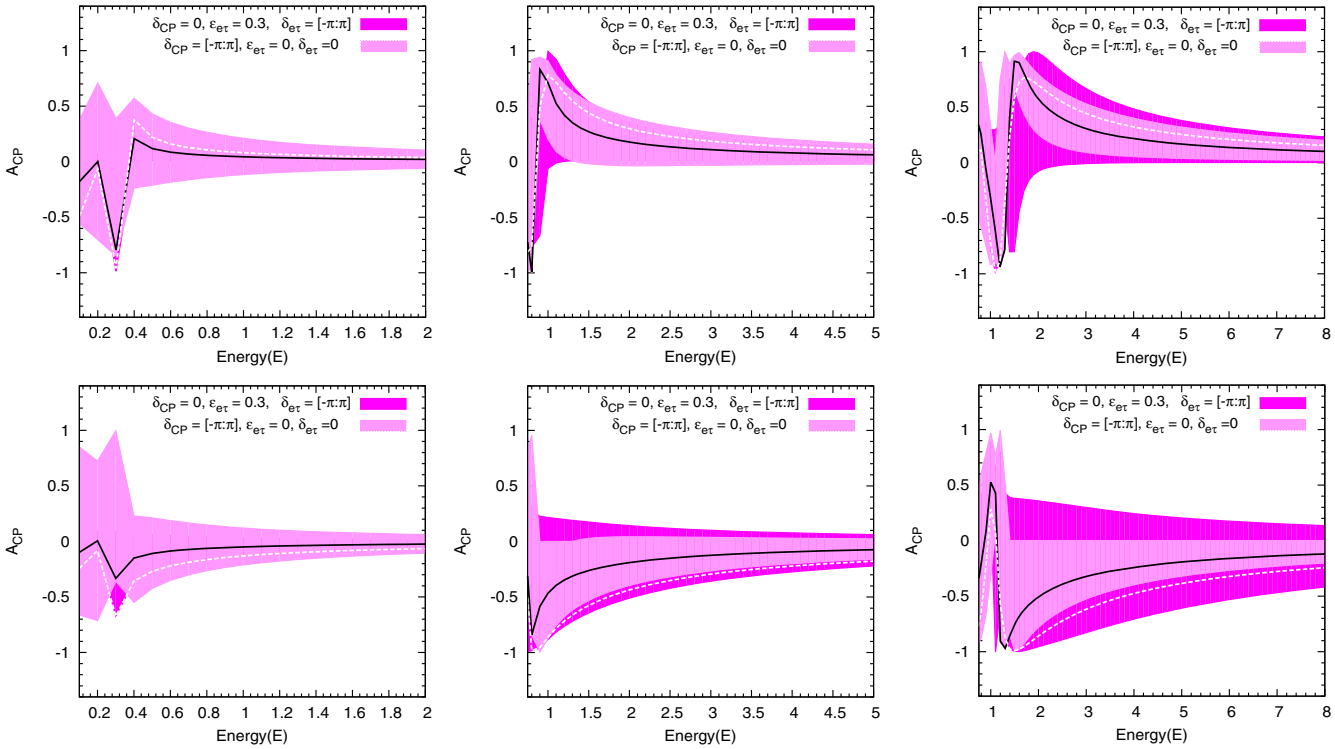

FIG. 6. The CP asymmetry bands for T2K (left panel), NOνA (middle panel), and DUNE (right panel) without NSI (light colored band) and with NSI (dark colored band) by assuming both NH (top panel) and IH (bottom panel). The solid black line corresponds to CP asymmetry for $\delta_{CP} = 0$ without NSI, whereas the dashed white line corresponds to CP asymmetry for $\delta_{CP} = 0$ with NSI ($\varepsilon_{e\tau} = 0.3$).

parameter and, therefore, it is very difficult to determine the CP violation in the presence of NSIs.

The CP violation sensitivity as a function of the true values of δ_{CP} for T2K (left panel), NOνA (middle panel), and DUNE (right panel) is shown in Fig. 7. The CP violation sensitivity is obtained by comparing the true event spectrum and test event spectrum with $\delta_{CP}^{\text{test}} = 0, \pi$. We do marginalization over the SO parameter space and add a prior on $\sin^2\theta_{13}$. From the figure, it is clear that there is a possibility to determine CP violation above 2σ, 3σ, and 5σ with 30%, 60%, and 60% of δ_{CP} parameter space for T2K, NOνA, and DUNE, respectively.

V. DEGENERACIES AMONG OSCILLATION PARAMETERS IN PRESENCE OF LFV-NSI

One of the major issues in neutrino oscillation physics is the parameter degeneracy among the oscillation parameters. In the standard oscillation physics, there are fourfold degeneracies among the oscillation parameters and they are known as octant degeneracy and mass hierarchy (sign of Δm^2_{31}) degeneracy. In this section, we present a simple way to understand the degeneracies among the oscillation parameters in the presence of the LFV-NSI parameter $\varepsilon_{e\tau}$, by using bi-probability plots, i.e., CP trajectory in a $P_{(\nu_\mu \to \nu_e)} - P_{(\bar{\nu}_\mu \to \bar{\nu}_e)}$ plane and $\delta_{CP} - A_{CP}$ plane.

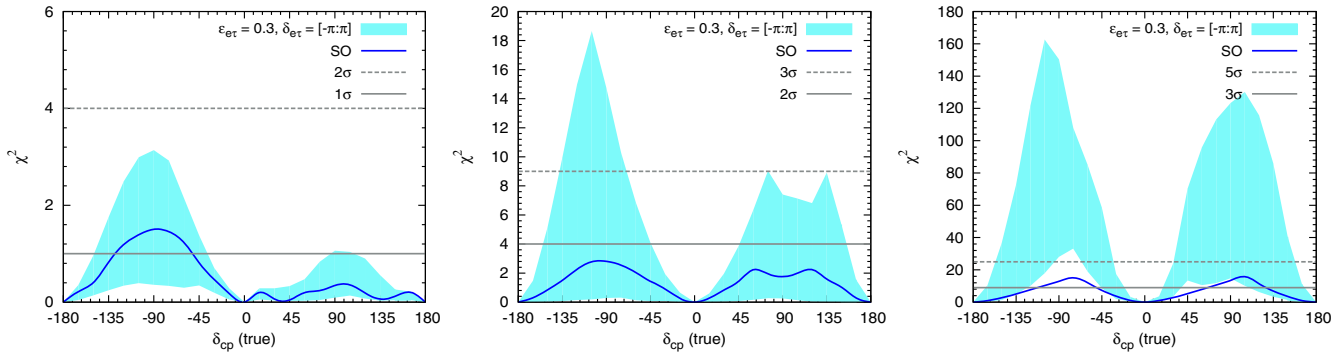

FIG. 7. The CPV potential as a function of true values of δ_{CP} for T2K (left panel), NOνA (middle panel), and DUNE (right panel) without NSI (solid blue line) and with NSI (band).

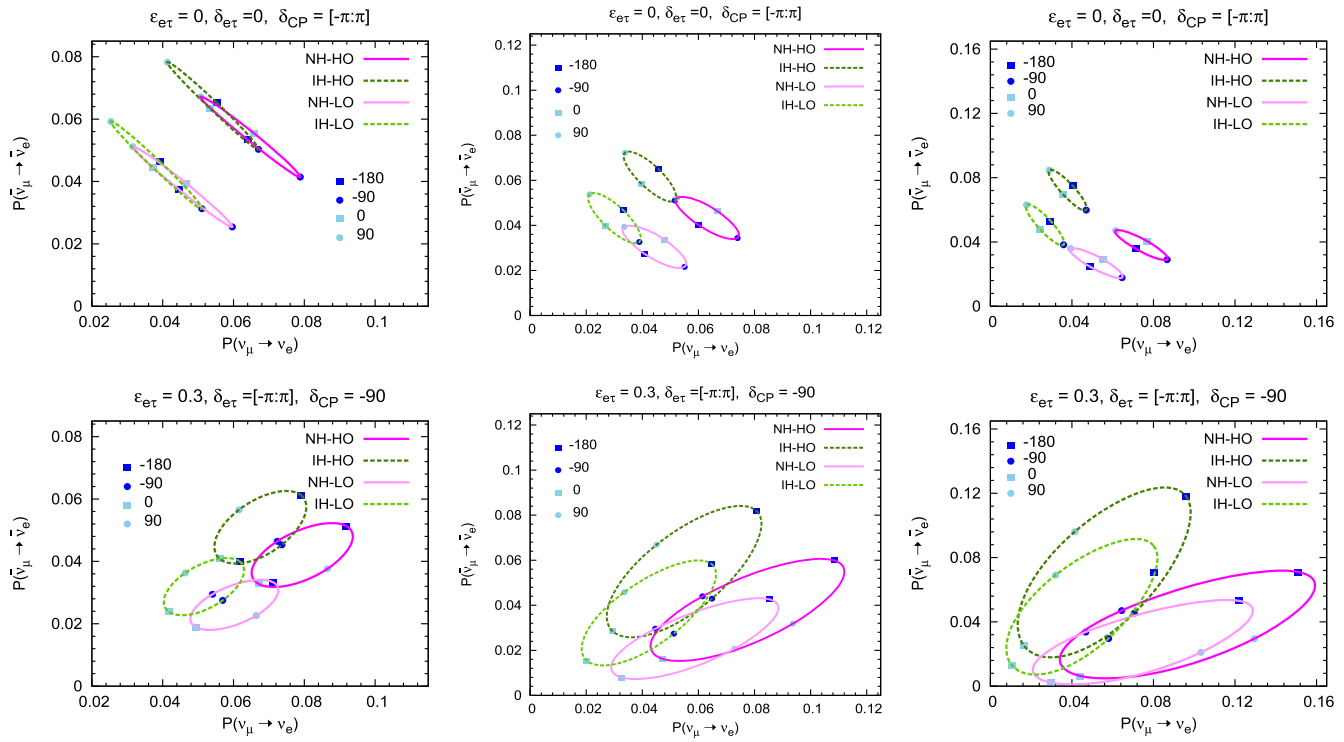

FIG. 8. The *CP* trajectory for T2K (left), NOνA (middle) and DUNE (right) with (bottom panel) and without (top panel) NSIs.

In Fig. 8, we show the bi-probability plots for T2K ($E = 0.6$ GeV, L = 295 km), NOνA ($E = 2$ GeV, L = 810 km) and DUNE ($E = 3$ GeV, L = 1300 km) for both NH (solid line) and IH (dashed line) where dark (light) color plot corresponds to HO (LO). In the figure, the upper panel corresponds to δ_{CP} trajectory without NSIs, whereas the lower panel corresponds to $\delta_{e\tau}$ trajectory with $\varepsilon_{e\tau} = 0.3$ and $\delta_{CP} = -90°$ (it is the presently favored value of the *CP* phase).

In the standard oscillation paradigm, the NH and IH ellipses are well separated in the case of the DUNE experiment, compared with the T2K and NOνA experiments. This means that the DUNE experiment has the highest mass hierarchy determination capability. However, the ellipses in the presence of LFV-NSI overlap with each other, which will significantly worsen the hierarchy determination capability of the DUNE experiment. It can also be seen from the figure that the octant degeneracy can be resolved by using all three experiments since the light colored ellipses are well separated from the dark colored ellipse in the SO, whereas the octant resolution capability of the NOνA and DUNE experiments worsen in the presence of LFV-NSI because there is significant overlap between the *CP* trajectories of HO and LO in the presence of LFV-NSI. Moreover, they present new types of degeneracies among oscillation parameters in the presence of LFV-NSI.

Now we focus on the bi-probability plot of DUNE with NSI (bottom right panel) in Fig. 8 for a detailed discussion on the resolution of parameter degeneracies among the oscillation parameters. One can see from the figure that

(i) If $\delta_{e\tau} = -180°$, then the points in the $P_{(\nu_\mu \to \nu_e)} - P_{(\bar{\nu}_\mu \to \bar{\nu}_e)}$ plane are well separated in the case of NH-HO and IH-HO, which is a clear indication of mass hierarchy determination even in presence of LFV-NSI. Whereas, the capability of MH is reduced in the case of IH-LO and NH-LO. It is also noted from the figure that NH(IH)-HO and NH (IH)-LO are also well separated, which means that octant determination is possible in this case.

(ii) If $\delta_{e\tau} = -90°$, then it is extremely difficult to infer any definitive conclusion about the determination of both mass hierarchy and octant, since all four degenerate points in the $P_{(\nu_\mu \to \nu_e)} - P_{(\bar{\nu}_\mu \to \bar{\nu}_e)}$ plane are very close to each other.

(iii) If $\delta_{e\tau} = 0$, then all four degenerate points are very close to each other in the $P_{(\nu_\mu \to \nu_e)} - P_{(\bar{\nu}_\mu \to \bar{\nu}_e)}$ plane, and, therefore, it is extremely difficult to make any decisive prediction about the determination of both mass hierarchy and octant.

(iv) If $\delta_{e\tau} = 90°$, then the points corresponding to NH-HO and IH-HO in the $P_{(\nu_\mu \to \nu_e)} - P_{(\bar{\nu}_\mu \to \bar{\nu}_e)}$ plane are very well separated, which is an indication of MH determination. However, the capability of the determination of the mass hierarchy is reduced in the case of LO. It is also noted that octant determination is poor in this case.

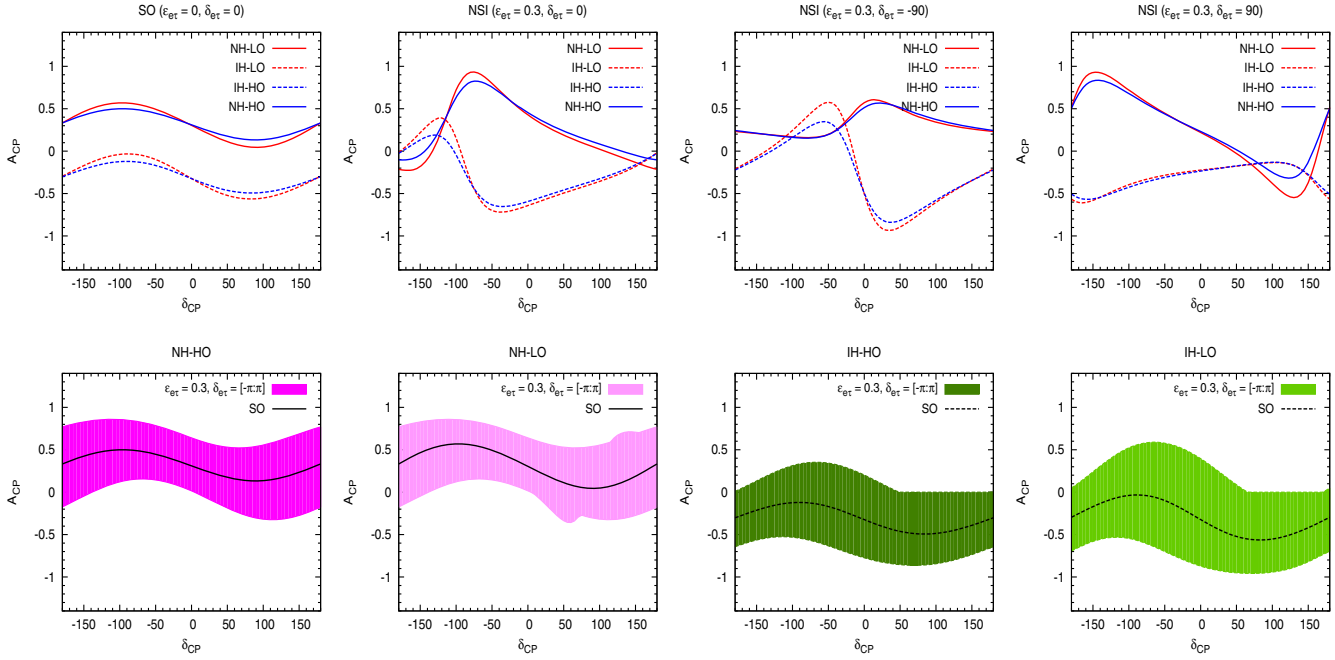

FIG. 9. The parameter degeneracy among the oscillation parameter in the δ_{CP}-CP asymmetry plane for the DUNE experiment. The top left panel shows the degeneracies in SO, whereas the other three panels show the degeneracy in the presence of LFV-NSI with $\delta_{e\tau} = 0$, -90, and 90, respectively. The bottom panel shows the A_{CP} for NH-HO, NH-LO, IH-LO, and IH-LO in the presence of NSI ($\varepsilon_{e\tau} = 0.3$ and $\delta_{e\tau} = [\pi : \pi]$).

All the above predictions are made under the assumption that the value of LFV-NSI $\varepsilon_{e\tau}$ is near to its upper bound and the value of the CP violating phase is near to its currently preferred value i.e., $\delta_{CP} = -90°$. Moreover, these predictions indicate that the mass hierarchy and octant determinations are possible even in the presence of LFV-NSI if $\delta_{e\tau} = -180°$ or 90°.

Another simple way to understand the parameter degeneracies among the oscillation parameters is by simply looking at the CP asymmetry, which is defined in

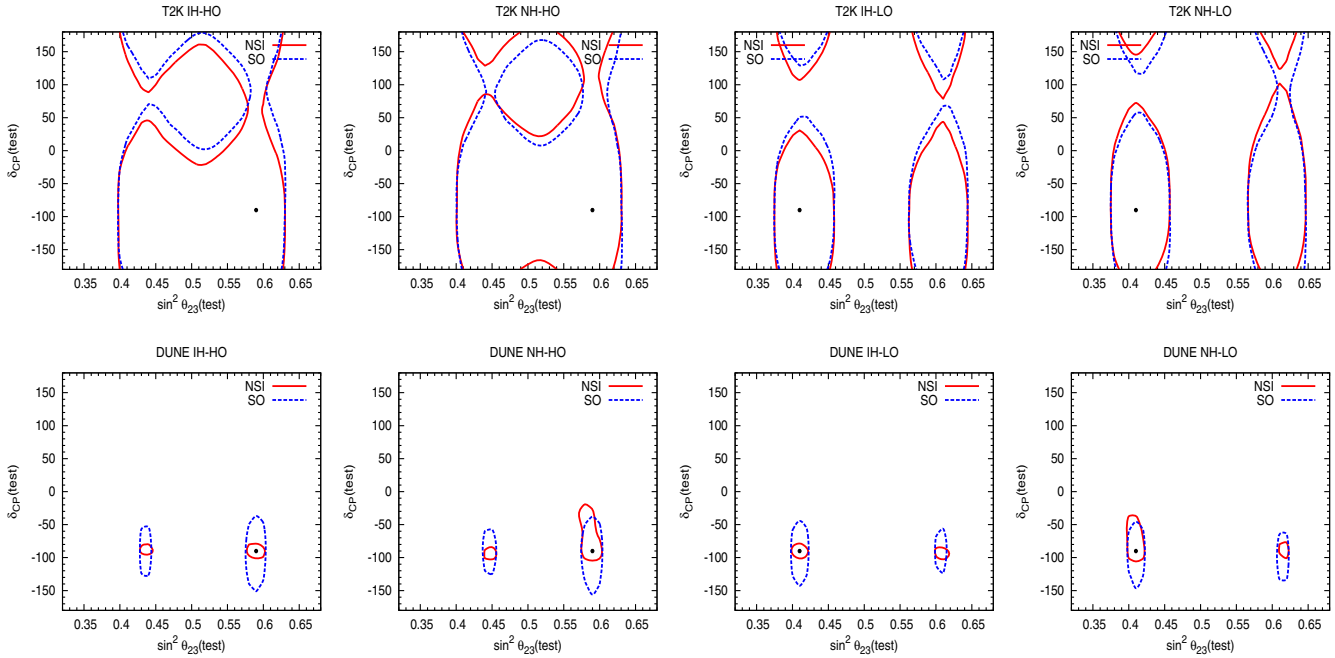

FIG. 10. The 2σ C.L. regions for $\sin^2\theta_{23}$ vs δ_{CP} with true $\sin^2\theta_{23} = 0.41$ (0.59) for LO (HO) and true $\delta_{CP} = -90°$. The top panel corresponds to T2K and the bottom panel corresponds to the DUNE experiments.

Eq. (7). CP asymmetry as a function of δ_{CP} for NH-LO, NH-HO, IH-LO, and IH-HO for the DUNE experiment is given in Fig. 9. The top left panel of the figure shows the CP asymmetry in standard oscillation, and it can be seen from the figure that CP asymmetry is more in LO than in HO for both NH and IH. The rest of the three in the top panel show the CP asymmetry in the presence of NSI with $\delta_{e\tau} = 0$, $-90°$, and $90°$, respectively. It is clear from the figure that LFV-NSI introduces other degeneracies among the standard oscillation parameters. Moreover, the bottom panel shows the A_{CP} for NH-HO, NH-LO, IH-LO, and IH-LO in the presence of NSI ($\varepsilon_{e\tau} = 0.3$ and $\delta_{e\tau} = [\pi : \pi]$). Therefore, degeneracy resolution in the presence of NSI is extremely complicated. It is also noted that the degeneracy resolution capability is mainly dependent on the value of $\delta_{e\tau}$; for instance, if $\delta_{e\tau} = 90°$, then the CP asymmetry for IH-LO and IH-HO are almost the same and one cannot distinguish between them.

A. Correlation between δ_{CP} and θ_{23}

In this section, we discuss the effect of LFV-NSI on the allowed parameter space of $\sin^2\theta_{23}$ and δ_{CP}. We show the 2σ C.L. regions for $\sin^2\theta_{23}$ vs δ_{CP} with true $\sin^2\theta_{23} = 0.41$ (0.59) for LO (HO) and true $\delta_{CP} = -90°$ in Fig. 10 for the T2K (top panel) and DUNE (bottom panel) experiments. From the figure, we can see that there is significant change in the allowed parameter space in the presence of LFV-NSI for DUNE.

VI. SUMMARY AND CONCLUSIONS

We have investigated the implications of LFV-NSIs on the physics potential of various neutrino oscillation experiments. We found that the discovery reach for the unknowns in oscillation physics by the experiments that we have considered can be altered significantly in the presence of LFV-NSIs. Moreover, we found that the degeneracy discrimination capability of all the experiments will worsen in the presence of LFV-NSI since it leads to new degeneracies among the oscillation parameters other than the existing degeneracies in standard oscillation physics. We also found that the possibility of misinterpretation of oscillation data in the presence of new physics scenarios (NSIs) gives rise to the wrong determination of the octant of the atmospheric mixing angle, neutrino mass hierarchy, and CP violation.

ACKNOWLEDGMENTS

We would like to thank the Science and Engineering Research Board (SERB), Government of India, for financial support through Grant No. SB/S2/HEP-017/2013.

[1] Y. Fukuda *et al.* (Super-Kamiokande Collaboration), Phys. Rev. Lett. **81** 1562 (1998).
[2] Q. R. Ahmad *et al.* (SNO Collaboration), Phys. Rev. Lett. **89**, 011301 (2002).
[3] K. Eguchi *et al.* (KamLAND Collaboration), Phys. Rev. Lett. **90**, 021802 (2003).
[4] K. Abe *et al.* (T2K Collaboration) Phys. Rev. Lett. **107**, 041801 (2011).
[5] Y. Abe *et al.* (DOUBLE-CHOOZ Collaboration), Phys. Rev. Lett. **108**, 131801 (2012).
[6] F. P. An *et al.* (DAYA-BAY Collaboration), Phys. Rev. Lett. **108**, 171803 (2012).
[7] J. K. Ahn *et al.* (RENO Collaboration), Phys. Rev. Lett. **108**, 191802 (2012).
[8] B. Pontecorvo, Sov. Phys. JETP **7**, 172 (1958).
[9] Z. Maki, M. Nakagawa, and S. Sakata, Prog. Theor. Phys. **28**, 870 (1962).
[10] F. P. An *et al.* (DAYA-BAY Collaboration), Phys. Rev. Lett. **108**, 171803 (2012).
[11] F. P. An *et al.* (DAYA-BAY Collaboration), Chin. Phys. C **37**, 011001 (2013).
[12] J. K. Ahn *et al.* (RENO Collaboration), Phys. Rev. Lett. **108**, 191802 (2012).
[13] M. Kuze (Double Chooz Collaboration), AIP Conf. Proc. **1441**, 461 (2012).
[14] L. Wolfenstein, Phys. Rev. D **17**, 2369 (1978).
[15] L. Wolfenstein, Phys. Rev. D **20**, 2634 (1979).
[16] S. Davison, C. Pena-Garay, N. Rius, and A. Santamaria, J. High Energy Phys. 03 (2003) 011.
[17] M. C. Gonzalez-Garcia and M. Maltoni, J. High Energy Phys. 09 (2013) 152.
[18] M. C. Gonzalez-Garcia, M. Maltoni, and J. Salvado, J. High Energy Phys. 05 (2011) 075.
[19] G. Mitsuka *et al.* (Super-Kamiokande Collaboration), Phys. Rev. D **84**, 113008 (2011).
[20] O. G. Miranda, M. A. Tortola, and J. W. F. Valle, J. High Energy Phys. 10 (2006) 008.
[21] A. Bolanos, O. G. Miranda, A. Palazzo, M. A. Tortola, and J. W. F. Valle, Phys. Rev. D **79**, 113012 (2009).
[22] A. Palazzo and J. W. F. Valle, Phys. Rev. D **80**, 091301 (2009).
[23] F. J. Escrihuela, O. G. Miranda, M. A. Tortola, and J. W. F. Valle, Phys. Rev. D **80**, 105009 (2009).
[24] A. Friedland, C. Lunardini, and C. Pena-Garay, Phys. Lett. B **594**, 347 (2004).
[25] H. Oki and O. Yasuda, Phys. Rev. D **82**, 073009 (2010).
[26] A. Bandyopadhyay *et al.*, Rep. Prog. Phys. **72**, 106201 (2009).
[27] D. Meloni, T. Ohlsson, W. Winter, and H. Zhang, J. High Energy Phys. 04 (2010) 041.

[28] A. M. Gago, H. Minakata, H. Nunokawa, S. Uchinami, and R. Zukanovich Funchal, J. High Energy Phys. 01 (2010) 049.
[29] J. Kopp, T. Ota, and W. Winter, Phys. Rev. D **78**, 053007 (2008).
[30] N. C. Ribeiro, H. Minakata, H. Nunokawa, S. Uchinami, and R. Zukanovich Funchal, J. High Energy Phys. 12 (2007) 002.
[31] M. Campanelli and A. Romanino, Phys. Rev. D **66**, 113001 (2002).
[32] P. Huber, T. Schwetz, and J. W. F. Valle, Phys. Rev. Lett. **88**, 101804 (2002).
[33] T. Ota, J. Sato, and N. Yamashita, Phys. Rev. D **65**, 093015 (2002).
[34] A. M. Gago, M. M. Guzzo, H. Nunokawa, W. J. C. Teves, and R. Zukanovich Funchal, Phys. Rev. D **64**, 073003 (2001).
[35] N. C. Ribeiro, H. Nunokawa, T. Kajita, S. Nakayama, P. Ko, and H. Minakata, Phys. Rev. D **77**, 073007 (2008).
[36] A. Esteban-Pretel, R. Tomas, and J. W. F. Valle, Phys. Rev. D **76**, 053001 (2007).
[37] H. Duan, G. M. Fuller, J. Carlson, and Y. Z. Qian, Phys. Rev. Lett. **97**, 241101 (2006).
[38] G. L. Fogli, E. Lisi, A. Mirizzi, and D. Montanino, Phys. Rev. D **66**, 013009 (2002).
[39] A. de Gouvea and K. J. Kelly, Nucl. Phys. **B908**, 318 (2016).
[40] P. Coloma, J. High Energy Phys. 03 (2016) 016.
[41] D. V. Forero and P. Huber, Phys. Rev. Lett. **117**, 031801 (2016).
[42] K. Huitu, T. J. Karkkainen, J. Maalampi, and S. Vihonen, Phys. Rev. D **93**, 053016 (2016).
[43] J. Liao, D. Marfatia, and K. Whisnant, Phys. Rev. D **93**, 093016 (2016).
[44] C. Soumya, K. N. Deepthi, and R. Mohanta, Adv. High Energy Phys., 141685 (2016).
[45] K. N. Deepthi, C. Soumya, and R. Mohanta, New J. Phys. **17**, 023035 (2015).
[46] M. Malinsky, T. Ohlsson, and H. Zhang, Phys. Rev. D **79**, 011301 (2009).
[47] T. Ohlsson, T. Schwets, and H. Zhang, Phys. Lett. B **681**, 269 (2009).
[48] C. Biggio, M. Blennow, and E. Fernandez-Martinez, J. High Energy Phys. 08 (2009) 090.
[49] G. Mitsuka *et al.*, Phys. Rev. D **84**, 113008 (2011); T. Ohlsson, Rep. Prog. Phys. **76**, 044201 (2013); P. Adamson *et al.* (MINOS Collaboration), Phys. Rev. D **88**, 072011 (2013); J. Kopp, P. A. Machado, and S. J. Parke, Phys. Rev. D **82**, 113002 (2010); S. Choubey, A. Ghosh, T. Ohlsson, and D. Tiwari, J. High Energy Phys. 12 (2015) 126.
[50] Y. Grossman, Phys. Lett. B **359**, 141 (1995).
[51] P. Huber, M. Lindner, and W. Winter, J. High Energy Phys. 05 (2005) 020.
[52] P. Huber, M. Lindner, T. Schwetz, and W. Winter, J. High Energy Phys. 11 (2009) 044.
[53] J. Kopp, Int. J. Mod. Phys. C **19**, 523 (2008); **19** (2008).
[54] J. Kopp, M. Lindner, T. Otta, and J. Sato, Phys. Rev. D **77**, 013007 (2008).
[55] P. Adamson *et al.* (MINOS Collaboration), Phys. Rev. Lett. **110**, 251801 (2013).
[56] P. Huber, M. Lindner, and W. Winter, Nucl. Phys. **B645**, 3 (2002).
[57] Y. Itow *et al.* (T2K Collaboration), arXiv:hep-ex/0106019.
[58] M. Ishitsuka *et al.*, Phys. Rev. **72**, 033003 (2005); K. Abe *et al.* (T2K Collaboration), Prog. Theor. Exp. Phys. **4**, 043C01 (2015).
[59] D. Ayres *et al.*, arXiv:hep-ex/0503053.
[60] R. Patterson, in *Proc. of Neutrino 2012 Conference*, June 3–9, 2012, Kyoto, Japan, http://neu2012,kek.jp/; P. Adamson *et al.* (NOvA Collaboration), Phys. Rev. Lett. **116**, 151806 (2016); Phys. Rev. D **93**, 051104 (2016).
[61] S. K. Agarwalla, S. Prakash, S. K. Raut, and S. U. Sankar, J. High Energy Phys. 12 (2012) 075.
[62] T. Akiri *et al.* (LBNE Collaboration), arXiv:1110.6249.
[63] LBNE Collaboration, http://lbne2-docdb.fnal.gov/cgi-bin/ShowDocument?docid=5823; R. Acciarri *et al.* (DUNE Collaboration) arXiv:1512.06148; arXiv:1601.05471.
[64] D. Forero, M. Tortola, and J. Valle, Phys. Rev. D **90**, 093006 (2014).
[65] H. Minakata, M. Sonoyama, and H. Sugiyama, Phys. Rev. D **70**, 113012 (2004).